

# RAIN GUTTER FRAGMENT – GREY CAST IRON – MODERN TIMES – FRANCE

<b>Artefact name</b>	Rain gutter fragment
<b>Authors</b>	Christian. Degriigny (HE-Arc CR, Neuchâtel, Neuchâtel, Switzerland) & Mathea. Hovind (University of Oslo, Department of archaeology, conservation and history (IAKH-UiO), Oslo, Oslo, Norway)
<b>Url</b>	/artefacts/1261/

## ∨ The object

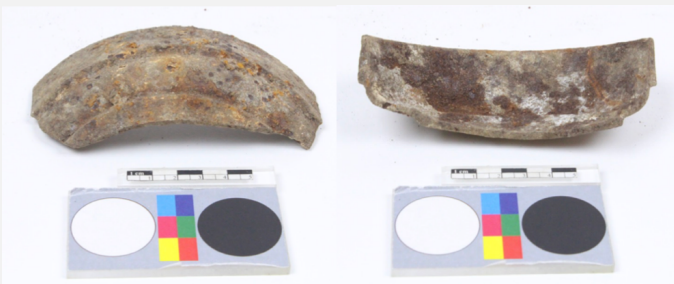


Fig. 1: Rain gutter fragment, exterior and interior faces (to the left and right, respectively),

*Credit UiO-IAKH, M.Hovind.*

## ∨ Description and visual observation

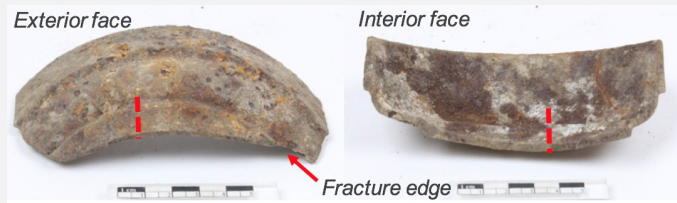
<b>Description of the artefact</b>	Rain gutter fragment (Fig. 1), possibly part of the extension of a roof drain pipe. Both the exterior and interior surfaces are covered by heterogeneous corrosion crusts. The underlying metal seems however to be well preserved, including features such as a difference in thickness etc. Dimensions: L = 55mm; W (interior) = 120mm; Tmax. = 6mm; WT = 176g.
<b>Type of artefact</b>	Architectural element
<b>Origin</b>	Château de Germolles (14th century), Mellecey, Bourgogne, France
<b>Recovering date</b>	Unknown
<b>Chronology category</b>	Modern Times
<b>chronology tpq</b>	<input type="text" value="1801"/> A.D. ▾
<b>chronology taq</b>	<input type="text" value="2000"/> A.D. ▾
<b>Chronology comment</b>	19th - 20th century
<b>Burial conditions / environment</b>	Outdoor atmosphere

Artefact location	HE-Arc CR, Neuchâtel, Neuchâtel
Owner	Château de Germolles, Mellecey, Bourgogne
Inv. number	None
Recorded conservation data	N/A

### Complementary information

None.

### Study area(s)



Credit UiO-IAKH, M.Hovind.

Fig. 2: The exterior and interior faces before sampling. The dotted line represents the sample location (a cross-section of the metal). The fracture edge corresponds to the edge that was formerly attached to the remaining artefact,

### Binocular observation and representation of the corrosion structure

The schematic representation below (Fig. 3) gives an overview of the strata encountered by visual macroscopic observation.

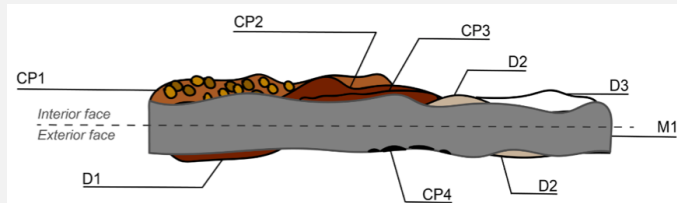


Fig. 3: Preliminary stratigraphy of the corrosion structure based on visual microscopic observation,

Captions	Description
D1	Scattered, orange to dark red encrustations. Probably corrosion products mixed with soil.
D2	Grey-brown and matte deposit, somewhat powdery - possibly corrosion product mixed with soil. This layer is located both on the interior and exterior surface of the artefact.
D3	Localized, white and strongly adherent deposit.
CP1	Bright orange to dark red corrosion product. Uneven surface with pustules.
CP2	Red-brown corrosion crust. Brittle, but adherent. Flakes off in bits when force is applied perpendicular to the surface with a scalpel.
CP3	Similar to CP2 but appears to be an individual layer.
CP4	Isolated corrosion blisters. Circular and black in colour. Mainly located on the exterior surface.
M1	Intact metal with a dark grey metallic sheen.

Credit UiO-IAKH, M.Hovind.

### MiCorr stratigraphy(ies) – Bi

## Sample(s)

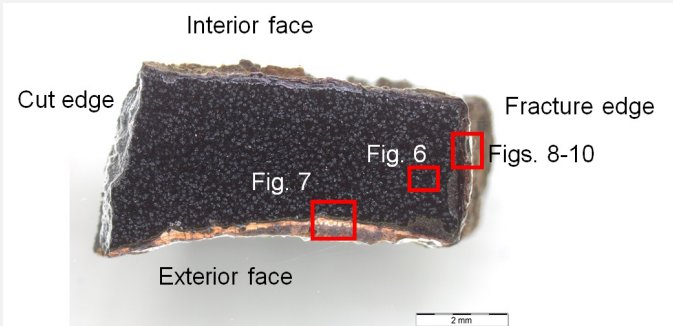


Fig. 4: Micrograph of the sample taken from the rain gutter fragment showing its orientation relative to the artefact and the locations of Figs. 6-10,

Credit UiO-IAKH, M.Hovind.

### Description of sample

The sample consists of a rectangular section (Fig. 4) which was cut out from the fractured edge of the gutter fragment. It is representative of three surfaces: the exterior and interior surface, as well as the fracture edge. Dimensions: L = 7mm; Wmax. = 5mm; Tmax. = 4mm (approx.).

Alloy	Grey cast iron
Technology	Cast
Lab number of sample	CIG2018 (Cast Iron Gutter, sampled in 2018)
Sample location	HE-Arc CR, Neuchâtel, Neuchâtel
Responsible institution	HE-Arc CR, Neuchâtel, Neuchâtel
Date and aim of sampling	March 2018, study of corrosion stratigraphy and chemical analyses

### Complementary information

The fact that the artefact was considered a test material enabled extensive sampling that would not otherwise be possible.

## Analyses and results

### Analyses performed:

Metallography: microscope: Leica DMI8 (a metallographic, inverted, reflected light microscope) with magnification up to 500X. Camera: Olympus SC50 connected to the software "Olympus Stream", version 1.9.4. Illumination modes: bright field and cross-polarized light.

SEM-EDS: instrument: Jeol 6400; voltage: 20 kV; working distance: 18 and 24mm; sample preparation: palladium depot.

## Non invasive analysis

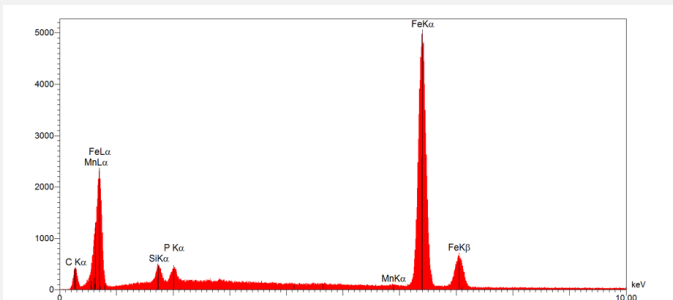
None.

The metal is a P-rich grey cast iron with Si and Mn (Fig. 5). Its microstructure is characterized by evenly distributed graphite flakes in a matrix composed of dendrites and an interdendritic eutectic phase (Fig. 6). What appears to be irregular graphite flakes / porosity is in fact deformed graphite flakes; graphite is soft and prone to destruction by smearing and/or preferential removal during polishing (Scott 1991).

The dendrites appear light grey under polarized light, while the eutectic phase appear light brown (Fig. 6). The eutectic phase is rich in Fe and P and contains small amounts of C and Si, whereas the dendritic phase contains much less P (Table 1).

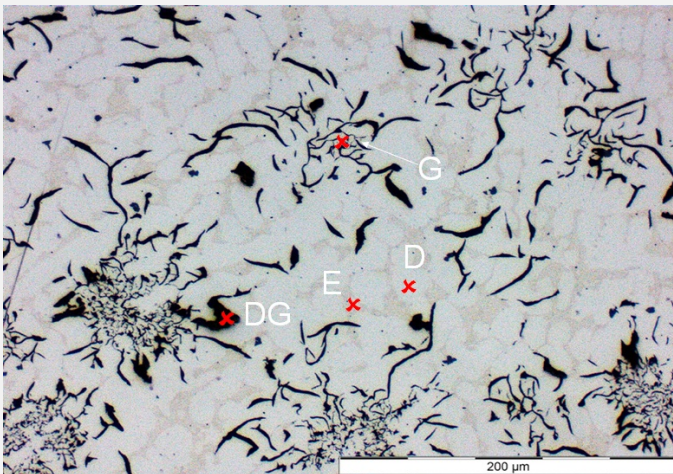
Elements mass %*	Fe	C	P	Si
<b>Phase</b>				
Eutectic phase	78	7	14	0.5
Dendritic phase	91	5	0.5	3

Table 1: Chemical composition of the matrix (eutectic and the dendritic phase). Method of analysis: SEM-EDS. Lab. of Electronic Microscopy and Microanalysis, Néode, HEI Arc, credit HEI Arc, C.Csefalvay. \* The value is the calculated average of three analyses of the same feature, but in different areas.



Credit HEI Arc, C.Csefalvay.

Fig. 5: EDS-spectrum showing the chemical composition of the metal. Method of analysis: SEM-EDS. Lab. of Electronic Microscopy and Microanalysis, Néode, HEI Arc,



Credit UiO-IAKH, M.Hovind.

Fig. 6: Micrograph of the metal sample from Fig. 4 (detail). Unetched, bright field. Graphite flakes (G) in black, the dendrites (D) in light grey and the eutectoid phase (E) in light brown. Deformed graphite (DG) flakes are visible as irregular black inclusions,

<b>Microstructure</b>	Dendritic structure with graphite flakes and a P-rich eutectic phase
<b>First metal element</b>	Fe
<b>Other metal elements</b>	C, Si, P, Mn

Complementary information

None.

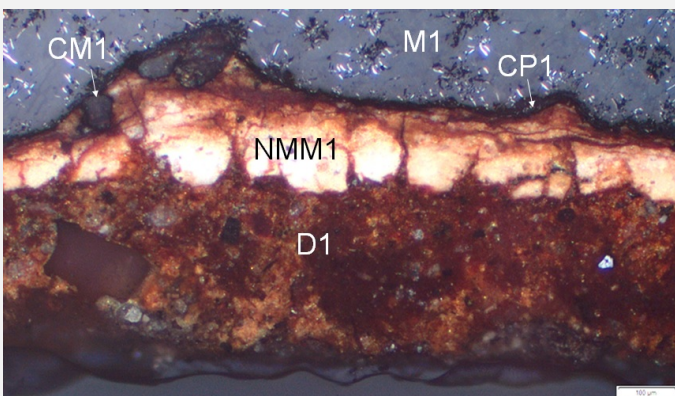
## Corrosion layers

The exterior face (Figs. 2, 4 and 7) consists of a white / light yellow cracked layer (NMM1 in Fig. 7) superimposed by a layer of deposit mixed with orange-red corrosion products (D1 in Fig. 7). Local analysis by SEM-EDS (Table 2) revealed that the white / light yellow layer is rich in Ba, O, S, Fe, C and Zn. It has a chemical composition similar to Lithopone ( $BaSO_4, ZnS$ ), a preparatory paint layer. Fe is probably a contamination from the superimposed porous deposit / corrosion product D1 (Table 2). The latter (D1) is Fe- and O-rich and contains Si, Al and some Ca, in addition to a range of elements (K, P, Na, Cl, S and Ti) present in minor amounts (Table 2). A thin layer of corrosion products (CP1) is located just beneath the paint layer, appearing dark grey under polarized light (Fig. 7). This layer is followed by a corroded metal phase (CM1). Their exact composition was not analyzed but is likely to correspond to the corroded metal phase of the fracture edge, described below.

The interior face (Figs. 2 and 4) shows similar characteristics but does not include a white layer similar to NMM1. The fracture edge however (Figs. 2, 4 and 8), shows a more complex stratigraphy consisting of a dense product layer which can be further divided into two individual strata (CP3 and CP2), superimposed by a porous corrosion crust appearing orange under polarized light (CP1) (Fig. 9). The corroded metal (CM1) is located just beneath CP3 and contains remnants of the P-rich eutectic phase (Figs. 8-10). The M/CP ratio (metal to corrosion products) is rather high, implying extensive internal corrosion. Furthermore, cracks are traversing the whole corrosion layers – indicating a fragilization of the structure. As for the composition of the corrosion products CP1, CP2 and CP3, they all contain Fe and O (Fig. 10). A marbling effect within CP2 and CP3 indicates a variation in the concentration of Fe and O (particularly visible in bright field - Fig. 8). The white deposit (D1 in Figs. 8 and 9) might originate from exposure to calcareous water (Table 2). The presence of exogenous elements such as Si, Ca, Al, Na and O (Table 2) was confirmed by elemental mapping (Fig. 10).

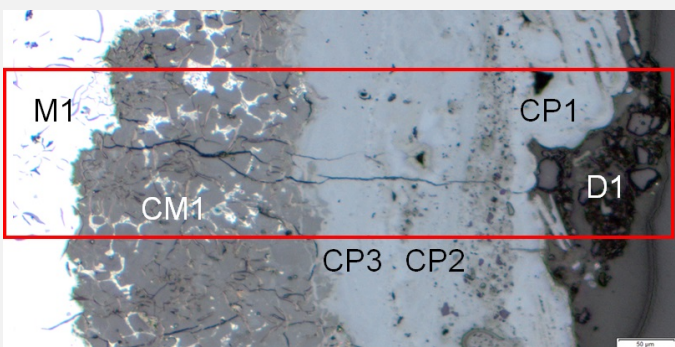
Elements mass %	Fe	O	Ba	C	Si	S	Zn	Al	Ca	P	K	Na	Cl	Ti
<b>Stratum</b>														
Deposit (D1)	22	34	-	26	10	<1	-	3	1	1	1	<1	<1	<1
Paint layer (NMM1)	10	23	37	9	0.5	12	7	-	1	-	-	-	-	-

Table 2: Chemical composition of the strata from Fig. 7. Method of analysis: SEM-EDS. Lab. of Electronic Microscopy and Microanalysis, Néode, HEI Arc, credit MiCorr\_HEI Arc, C.Csefalvay. \*The value is the calculated average of three analyses of the same feature, but in different areas.



Credit UiO-IAKH, M.Hovind.

Fig. 7: Micrograph of the metal sample from Fig. 4 (detail), unetched, polarized light, 5x. Stratigraphy of the exterior surface, to be compared to Fig. 11 and from top to bottom: the metal (M1) in grey, a layer of corroded metal (CM1) followed by a thin layer of CP1, and a white cracked layer (NMM1) superimposed by a porous dark-red deposit (D1),



Credit UiO-IAKH, M.Hovind.

Fig. 8: Micrograph of the metal sample from Fig. 4 (detail), unetched, bright field. Stratigraphy of the fracture edge, to be compared to Fig. 12 and from left to right: intact metal (M1) in white, followed by preferentially corroded metal (CM1) and dense product layers (CP3 and CP2) in various shades of grey. CP1 is slightly porous and covered by grain-like particles (D1). The area selected for elemental chemical distribution (Fig. 12) is marked by a red rectangle,



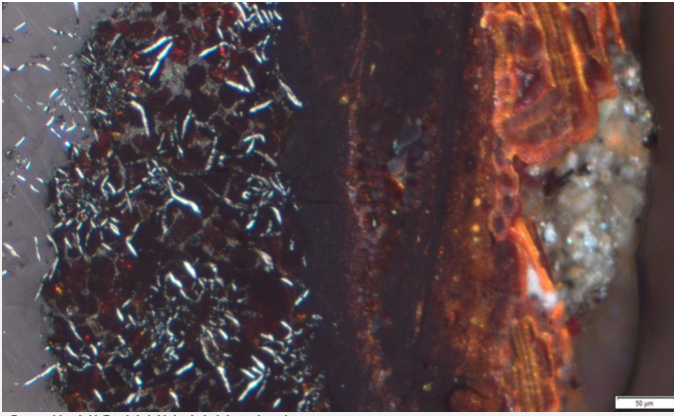


Fig. 9: Micrograph similar to Fig. 8 but under polarized light. The external deposit (D1) appears grey-white, CP1 in bright orange, while CP2 and CP3 appear dark red to brown. The corroded metal (CM1) contains remnants of graphite flakes (in white) and the P-rich eutectic (in grey),

Credit UiO-IAKH, M.Hovind.

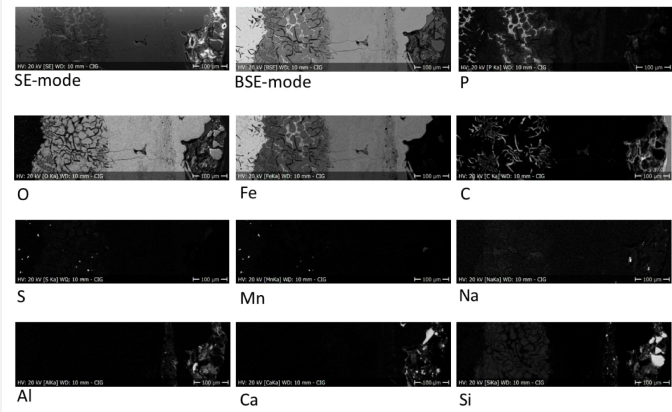


Fig. 10: SEM image and elemental chemical distribution of the selected area from Fig. 8. Method of analysis: SEM-EDS. Lab. of Electronic Microscopy and Microanalysis, Néode, HEI Arc,

Credit HEI Arc, C.Csefalvay.

<b>Corrosion form</b>	Multiform
<b>Corrosion type</b>	Unknown

Complementary information

None.

∨ MiCorr stratigraphy(ies) – CS

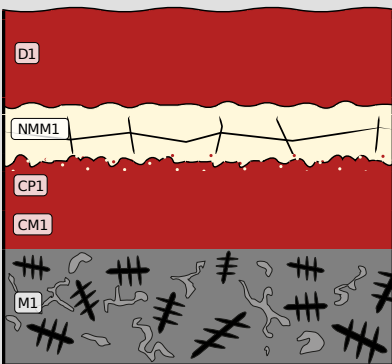
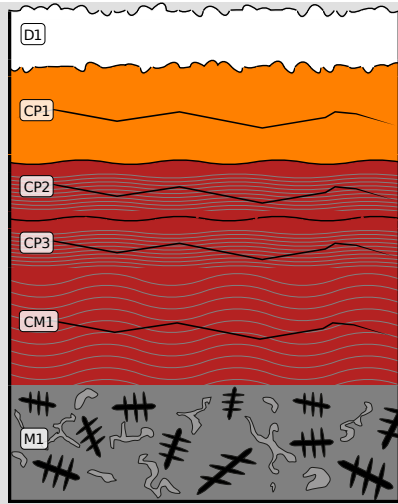


Fig. 11: Stratigraphic representation of the sample taken from the rain gutter fragment in cross-section (dark field) using the MiCorr application. The characteristics of the strata are only accessible by clicking on the drawing that redirects you to the search tool by stratigraphy representation. This representation can be compared to Fig. 7 (exterior surface). CP1 corresponds to CP2 in Fig. 3, Credit UiO-IAKH, M.Hovind.

Fig. 12: Stratigraphic representation of the sample taken from the rain gutter fragment in cross-section (dark field) using the MiCorr application. The characteristics of the strata are only accessible by clicking on the drawing that redirects you to the search tool by stratigraphy representation. This representation can be compared to Figs. 8 and 9 (fracture



edge). D1 corresponds to D3 in Fig. 3, Credit UiO-IAKH, M.Hovind.

### ✓ Synthesis of the binocular / cross-section examination of the corrosion structure

The schematic representation of corrosion layers integrating additional information based on the analyses carried out is given in Fig. 13.

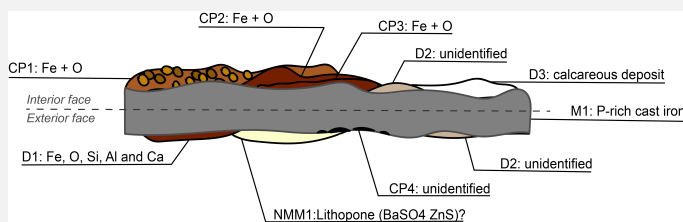


Fig. 13: Improved stratigraphic representation of the rain gutter fragment based on analysis from cross-section and visual microscopic observation,

Credit UiO-IAKH, M.Hovind.

### ✓ Conclusion

The rain gutter fragment is a grey cast iron with a microstructure consisting of graphite flakes and a P-rich eutectic phase. The corrosion layers of the exterior surface contains a preparatory paint layer, located beneath a layer of iron corrosion products mixed with soil. It seems likely that the cast iron gutter has been covered with a protective paint layer (e.g. Lithopone) to slow down the rate of atmospheric corrosion. The presence of Lithopone reinforces the suggested dating of the artefact (20th century) as this pigment was developed and used from the 1880s and onwards (Lithopone 2007). However, it seems that the protective layer has none or only very limited effect as (pitting) corrosion is present also in these areas.

The corrosion layers consist mainly of Fe and O, indicating atmospheric corrosion with presence of only a very small amount of contaminants/pollution. The scattered white deposit is possibly originating from exposure to calcareous water as it is localized mainly on the interior face of the fragment, where rain water would hit the metal before entering the ground.

### ✓ References

#### References on object and sample

##### References sample

1. Scott, D. A. (1991) Metallography and microstructure of ancient and historic metals. Marina del Rey, Calif:

Getty Conservation Institute in association with Archetype Books, 38-39.

2. Lithopone (2007) In: Gooch J.W. (eds) Encyclopedic Dictionary of Polymers. Springer, New York, NY.